Thermochimica Acta, 18 (1977) 43–71

THERMAL TECHNIQUES IN BIOMEMBRANE AND LIPOPROTEIN RESEARCH*

DONALD L. MELCHIOR, FRANCIS J. SCAVITTO, MARY T. WALSH AND JOSEPH M. STEIM**

Department of Chemistry, Brown University, Providence, Rhode Island 02912 (U. S. A.)

ABSTRACT

In structural determinations of inanimate materials, thermal analysis has long proven to be a powerful technique, particularly when coupled with X-ray diffraction or spectroscopic methods. In molecular biology, thermal analysis, frequently combined with other techniques, similarly shows itself to be a powerful tool. Its importance is not limited solely to understanding biological structures but extends to understanding physiological processes as well.

This paper describes the application to molecular biology of differential scanning calorimetry (DSC) and the complementary technique of differential scanning dilatometry (DSD). The modification and operation of two commercial differential scanning calorimeters for use in molecular biology is discussed, as well as the design and operation of a novel differential scanning dilatometer together with its auxiliary techniques. Some examples are given of the uses of these methods in understanding the structure, thermodynamic state, and physiological functions of biological membranes.

A further illustration of the type of approach taken in applying thermal analysis to molecular biology is provided by a description of an ongoing study. This study uses DSC and DSD in correlation with the temperature dependence of ultraviolet circular dichroism (CD) to elucidate the structures of human high density (HDL) and low density (LDL) serum lipoproteins.

INTRODUCTION

Without doubt, the single most important contribution of thermal analysis to molecular biology has been to establish the lipid bilayer as the fundamental structure of biological membranes. As early as 1899, studies on the permeability of cell surfaces to lipid-soluble substances suggested that these membranes have a predominately lipid nature[1]. In 1925, studies using the newly developed Langmuir trough led to the

*Presented at the 6th North American Thermal Analysis Society Conference, Princeton, N. J., June 20–23, 1976.

**To whom requests for reprints should be sent.

hypothesis that biological membranes were bilayers of lipid molecules[2]. In the following years, the basic model of biological membranes as lipid bilayers with associated protein was developed[3]. This model was supported by studies using X-ray diffraction[4] and electron microscopy[5]. In the middle 1960's, researchers influenced by the developments and successes of protein chemistry questioned the bilayer concept of biomembranes[6–9]. It was suggested that biological membranes were composed of various types of protein subunits with more or less tightly associated lipid as opposed to a continuous lipid bilayer with associated protein. At this point, the development of the techniques of DTA and DSC and their application to lipid bilayer systems set the stage for a conclusive demonstration of the correctness of the bilayer concept.

THE THERMAL BEHAVIOR OF LIPID BILAYERS IN EXCESS WATER

In order to understand the thermal behavior of biological membranes, it is necessary to consider the behavior of membrane polar lipids in water. To a first approximation these lipids all have the same structure: two long-chain hydrocarbons bonded in some manner to a polar moiety. When suspended in water they associate to produce a variety of supramolecular systems whose conformations depend upon past history, temperature, concentration, and the nature of the lipid molecules themselves[10]. At physiological temperatures and excess water (i.e., more added water does not alter the state of lipid) the preferred conformation is the bilayer for naturally-occurring mixtures and even for pure phospholipids. These bilayers exist as liquid-crystalline particles formed from many concentric bilayer sheets (lamellae) with each sheet separated from its neighboring sheet by a layer of interstitial water[11]. The particles do not coalesce when in contact with one another, and, like other liquid crystalline systems, are birefringent.

The property of lipid bilayers which is particularly amenable to thermal analysis is a reversible, thermally-induced transition from an ordered crystalline-like

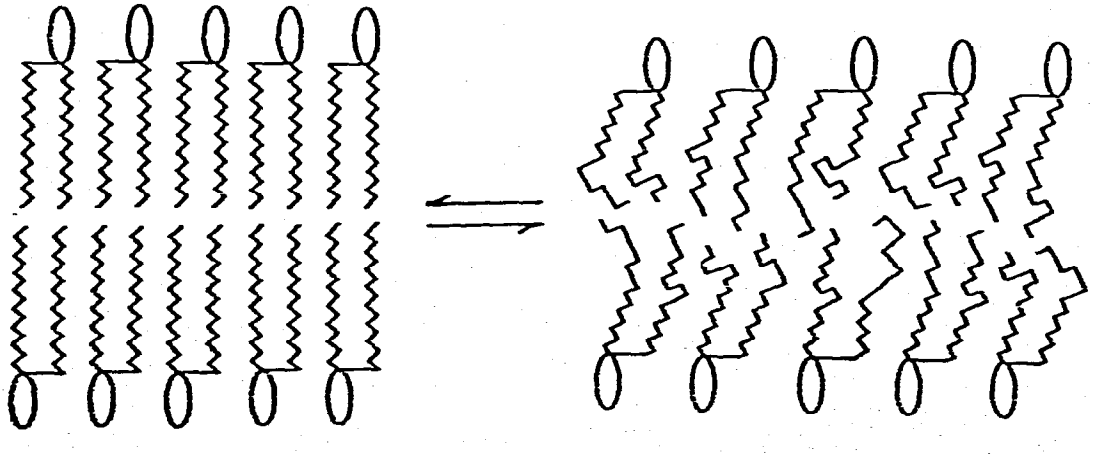

Fig. 1. The order/disorder transition in a phospholipid with uniform fatty acid chains.

state at low temperatures to a disordered fluid state at higher temperatures (Fig. 1). It is not accompanied by a rearrangement of the bilayer to a different liquid-crystalline system. It is, instead, a melting of the bilayers themselves, with the lamellar conformation conserved throughout the process. On a molecular level it consists of a change in the lipid hydrocarbon chains from a largely all-trans conformation to a more disordered state, accompanied by a lateral expansion and decrease in the thickness of the bilayer[12].

The melting temperatures are dependent upon the nature of the polar hydrophilic portion of the lipid molecules and especially upon the nature of the hydrocarbon chains (Fig. 2). Introduction of double bonds, for example, drastically reduces the transition temperature just as it does in fatty acids and pure hydrocarbons[13]. Since the lipid molecules within the bilayer are free to diffuse laterally above the transition temperature, systems containing mixed lipids with different melting points produce broad transitions in which fractional crystallization can occur in the plane of the bilayer[14].

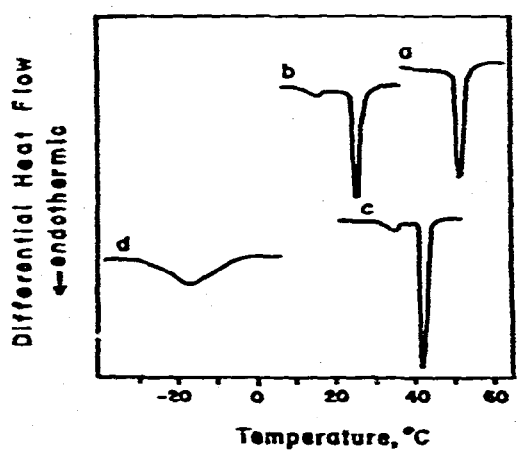

Fig. 2. DSC scans of phospholipids in excess water, showing (a) dipalmitoyl phosphatidylethanolamine; (b) dimyristoyl lecithin; (c) dipalmitoyl lecithin; (d) egg lecithin. Ethylene glycol was added to (d) as an antifreeze. The smaller, lower temperature "premelts" in (b) and (c) are a characteristic only of lecithins.

DSC AND THERMOTROPIC TRANSITIONS IN BIOMEMBRANES

Figure 3 shows a DSC study performed on *Acholeplasma laidlawii*. This microorganism, particularly well suited for membrane studies, was the first cell whose membrane was shown to undergo the lipid order/disorder transition[15]. The thermal events occurring in the *A. laidlawii* membrane are common to the membranes of many other organisms. Two endotherms occur when scanning up in temperature. The lower-temperature endotherm is nearly the same in living organisms, membrane preparations, and aqueous dispersions of extracted membrane lipids. It is reversible, and as judged by calorimetry, is almost unaffected by thermal protein denaturation,

enzymatic digestion of the membranes, or even by the absence of protein[16–18]. By analogy with synthetic phospholipids it was suggested[16] that the transition is essentially the same as the order/disorder transition seen in phospholipids in water and as such constituted direct evidence of the presence of a bilayer. This interpretation was later confirmed by X-ray diffraction[19]. By comparison of heats of transition of membranes with their extracted lipids, it was further suggested that 90±10% of the membrane lipids exist in the bilayer conformation[16]. This estimate was also later verified by other techniques[19,20]. This demonstration of a phenomenon involving the cooperative behavior of a majority of the membrane lipids melting as a bilayer eliminated membrane models based on protein subunits with associated lipids.

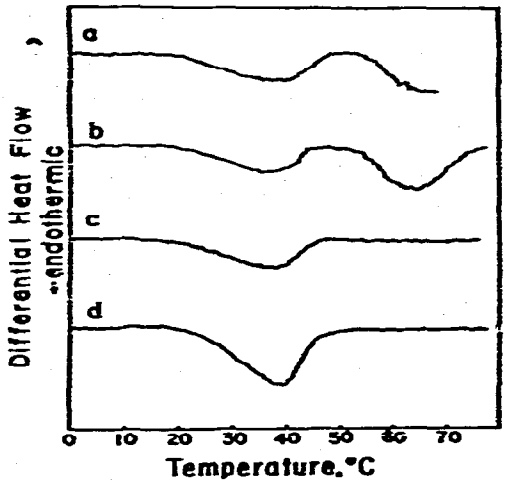

Fig. 3. DSC scans of *A. laidlawii*. (a) Whole cells; (b) membranes before protein heat denaturation; (c) membranes after protein heat denaturation; (d) extracted membrane lipids. All samples were taken from the same culture of cells grown in tryptose medium at 37°C, and run in a modified Perkin-Elmer DSC-1B.

The high temperature endotherm observed in Fig. 3 is irreversible and arises from protein denaturation. Its position is invariant with fatty acid composition, even though the position of the reversible lipid endotherm can be varied by as much as 70°C (from −20 to +50°C) by causing *A. laidlawii* to incorporate different fatty acids into its membrane lipids. The assignment of the second peak to irreversible protein denaturation was made by circular dichroism[21].

Although the initial importance of thermotropic transitions occurring in biological membranes was the insight they gave into the structure of the membrane matrix, more recent research has emphasized their physiological implications and has explored their use as a means of understanding lipid–protein associations[22]. Figure 4 shows some representative DSC scans of various biological membranes. Such transitions occur over broad temperature ranges, starting and ending gradually. Although spectroscopic and X-ray diffraction techniques are very valuable in understanding the molecular events which occur during such transitions, their overall course is probably

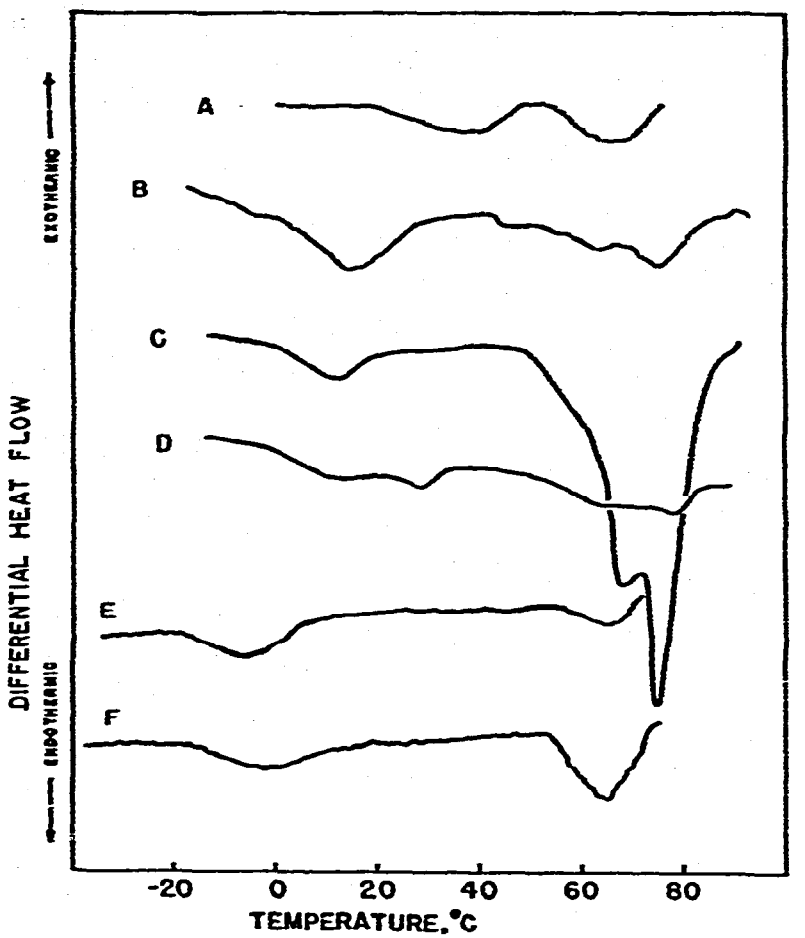

Fig. 4. DSC scans of biomembrane transitions, all obtained with 50% ethylene glycol as an anti-freeze. (A) *Acholeplasma laidlawii* membranes from cells grown in tryptose medium at 37°C; (B) *Micrococcus lysodeikticus* membranes from cells grown in brain-heart infusion at 37°C; (C) *Escherichia coli* K12 W945 whole cells grown in minimal salts with glucose at 20°C; (D) same cells as in (C), but scanned after thermal protein denaturation; (E) rat liver microsomes; (F) rat liver mitochondria. In all cases a lower-temperature reversible lipid transition is followed by a higher, temperature irreversible protein peak. The protein denaturation peaks are featureless in (A), (E), and (F), but show fine structure in (B), (C), and (D). Unlike other organisms, *E. coli* after heating shows two lipid transitions and residual reversible protein denaturation seen in (D). All scans shown were obtained by a modified Perkin-Elmer DSC-1B.

best described by thermodynamic methods. Because of experimental constraints imposed by the system itself, some thermodynamic parameters are not as readily measurable as they are in more conventional materials. But the heat of transition is an important parameter that can be readily measured by differential scanning calorimetry. A peak is recorded whose shape faithfully reflects the extent of the transition as a function of temperature. Since it is sensitive to very minor changes in the position and shapes of peaks, the scanning calorimeter is capable of describing the thermal properties of biomembranes in richer detail than can be obtained from

other methods. Dilatometry, the measurement of volume change, is another thermodynamic method which has been applied to the problem. Its use to date has been restricted to only a few studies, but, as will be discussed, it is potentially a valuable complement to calorimetry and in some cases can yield information not obtainable by calorimetry.

Certain features are characteristic of the materials and phenomenon studied by calorimetry in molecular biology. Thermal events such as bilayer transitions and protein denaturation are broad, ill defined, and not very energetic. The enthalpy of the order/disorder transition in membrane bilayers is between 1 and 10 cal g^{-1} of membrane lipid; the enthalpy of denaturation of ribonuclease is about 7 cal g^{-1}. In comparison, the enthalpy of fusion of n-paraffins is about 35 cal g^{-1}. Order/disorder transitions in biomembranes can occur over a temperature range as broad as 30 to 40°C, starting and ending very gradually. Often these transitions occur at temperatures as low as −30 or 40°C. Protein denaturation often occurs at temperatures as high as 90°C plus. The biological materials themselves are often difficult to obtain and the water present in the specimen limits the amount of sample that can be investigated. For example, a typical membrane preparation of sedimented pellet is 90% water, 5% membrane protein, and 5% membrane lipid. Thus, a typical 100 mg sample will contain only 5 mg of the material of interest.

As a consequence of these facts, a differential scanning calorimeter suited for molecular biological studies requires certain features: it should require small samples, and it should have high sensitivity, small signal-to-noise ratio, and a very steady baseline. It should operate at temperatures from at least −40 to 100°C. Due to the instability of many membrane model systems below their melting temperature, the ability to perform downscans is very useful. No instrument commercially available adequately satisfies all these requirements. Adequate results have been obtained using a DSC offered by DuPont which is fundamentally a differential thermal analyzer rather than a true scanning calorimeter. We have found that very excellent results can be obtained by modifying two other commercially available instruments.

MODIFICATION OF THE PERKIN-ELMER DSC-1B

The modification and operation for biomembrane studies of the Perkin-Elmer DSC-1B has been described in detail elsewhere[23,24]. The modifications have two aspects: (1) modifications to optimize the signal-to-noise ratio at low temperatures; (2) modifications to allow the use of large samples.

Modifications for subambient temperatures

As received from the manufacturer, the DSC-1B is equipped for low-temperature work. A Dewar flask filled with liquid nitrogen or dry ice and alcohol is placed over the sample holders to provide a low-temperature heat sink. However, the sample analyzer assembly containing the sensors and heaters is mounted on a chassis where the underside is exposed to the atmosphere. Unfortunately, this cools not only the

sample analyzer but the chassis as well. Condensation of water, and even the formation of ice, on the underside of the chassis wets the electrical components and causes baseline instability and noise after extended operation. Furthermore, the heat sink is so closely coupled to the analyzer that the addition of extra liquid nitrogen or the settling of dry-ice chips can cause shifts in the baseline.

These problems can be averted by minor modifications in the analyzer. The entire analyzer head is unplugged from the chassis of the analyzer module and inserted into a massive brass cylinder (outer diameter 4.50 in., height 5.50 in., wall thickness 0.50 in.) provided with an octal socket to receive it. A brass top is held with six screws and sealed with an O-ring. The cylinder is continuously purged with dry nitrogen, which enters through a copper tube at the bottom and exits at the top. It is immersed in a low-temperature alcohol bath cooled by a condensing unit charged with Freon 22. The bath has a volume of 16 l and is well agitated.

Sample pan design

The presence of water in biological materials requires that the sample pans be sealed. Sealable pans are available from Perkin-Elmer. They are useful for energetic transitions in synthetic phospholipids where as little as 1 mg of lipid will sometimes suffice, but for biomembranes their small volume (about 15 μl) is inadequate. For membrane samples, volumes of 100 μl are often necessary; for whole cells 200 μl is desirable. The problem of pan design, which might be expected to be trivial, is in fact complicated by several factors. Pans must be of low mass so that the heaters are not overloaded. They must present a minimum surface in order to minimize radiation. They must be easily and quickly sealed and just as easily opened to allow removal of the sample. They must withstand heating to about 100°C without leaking. Excellent results are obtained with a simple pillbox style pan. The bottom is machined of brass and gold-plated with walls approximately 0.01–0.02 in. thick, and an outside diameter of 0.268 in. Its height can be variable, but typically is 0.175 in. ($\sim$100 μl volume). The lid is punched aluminium, and is in reality a Perkin-Elmer dry sample pan. The bottom is provided with a 2° taper, so that when the lid is forced on, its sides expand slightly to make it fit snugly. The entire assembly is then sealed with Eastman 910*, a cyanoacrylate adhesive. With these large sample pans serious convective disturbances can occur if the viscosity of the samples is low. Convection is not a problem in sedimented pellets of biomembranes, but references of water or aqueous salt solutions must include a thickening agent such as 1–2% Sephadex G-200. Baseline curvature depends upon many factors, including the size, shape, and emissivity of the pans; and the mass, thermal conductivities, and heat capacities of the sample and reference. Every effort should be made to match the sample and reference as closely as possible, but nevertheless curvature can never be completely eliminated. Remaining curvature can be controlled by placing a spot of flat black paint (trial and error) on either the sample pan or reference pan to adjust emissivities.

*Eastman Kodak Co., Rochester, N.Y.

With the above modification, and proper sample handling and calorimeter operation[23,24], one can obtain excellent scans using 100 μl samples with a scan rate of 5°C min^{-1} at the instrument's highest sensitivity setting of 1 mcal sec^{-1}. Indeed, the scans are noiseless enough to permit the maximum sensitivity of the calorimeter to be effectively doubled by setting the chart recorder to a 5 mV input instead of the suggested 10 mV input. The scans of biomembrane transitions shown in Fig. 4 were all obtained on a modified DSC-1B.

MODIFICATION OF THE PERKIN-ELMER DSC-2

In addition to the DSC-1B, Perkin-Elmer has developed a newer instrument, the DSC-2. According to the manufacturer this instrument is a considerable improvement over the DSC-1B in terms of facility of use, improved signal-to-noise ratio, reduction of baseline curvature, choice of scan rates, and operation at subambient temperatures. We have found that modifications similar to those described for the DSC-1B are necessary before the DSC-2 can be used in its most sensitive mode[25] of 0.1 mcal sec^{-1}.

Although the modified DSC-1B using 100-μl sample pans has about the same capacity to sense small thermal events as the modified DSC-2, the DSC-2 has certain definite advantages. The modified DSC-2 has adequate sensitivity for studying transitions in biomembranes and related phenomena using commercial 15-μl sample pans. In comparison to the 100-μl sample pans, use of the small pans not only requires less sample, but their smaller size effectively eliminates temperature gradients within the pans and poor time response. Specimens can be scanned at a rate of 10°C min^{-1}. The small pans are more quickly and conveniently loaded than the large pans and have a smaller likelihood of leaking at higher temperatures. For subambient operation the DSC-2 is used in conjunction with a dry box, which greatly speeds up loading successive samples.

Although the environmental isolation of the DSC-2 is greatly improved compared to the DSC-1B, it is nevertheless still not adequate for operation of the instrument on the more sensitive ranges. In order to satisfactorily isolate the DSC-2 detector from the environment, two modifications must be made: improved thermal isolation and improved mechanical isolation.

For low-temperature operation, two types of cooling mechanisms are commercially available: (1) "intracoolers", a refrigeration unit coupled to an expansion chamber contained in a brass plate which fastens directly to the DSC-2 sample holder block; (2) a subambient accessory consisting of an aluminum cold finger fastened to the sample holder block and immersed in a reservoir of liquid nitrogen. Although with neither of these accessories are the detectors adequately isolated thermally from the environment, the intracoolers are the least satisfactory of the two.

In the DSC-2 the sample holders are symmetrically mounted in an aluminum block. When the intracooler is installed, a brass plate is attached to the sample holder. This brass plate has the expansion chamber of the refrigeration system asymmetrically located within it. This arrangement is a source of noise because the thermal

fluctuations which continually occur within the plate are not averaged out before they are encountered by the holders. Additional noise occurs because the efficiency of the small air-cooled refrigeration unit varies with ambient room temperature. This variance is readily detected on the more sensitive ranges. An attempt to improve the intracooler system by replacing the small air-cooled refrigeration unit with a larger water-cooled unit helped, but the results were still not satisfactory.

The cold finger with liquid nitrogen reservoir provided better results than the unimproved intracooler system. With it too, however, the DSC-2 output was noisy and showed correlations with room temperature. This accessory has the added disadvantage for routine use of requiring the reservoir be maintained with liquid nitrogen, a process both inconvenient and expensive. Further, although the temperature of the heat sink should be sufficiently low, too large a difference between sample and heat sink introduces unnecessary baseline curvature. A 25°C differential is desirable.

Since biomembranes frequently require scans be performed from about −40°C, a heat sink maintained at −65°C is more desirable than the −196°C of liquid nitrogen.

In addition to inadequate thermal isolation, the DSC-2 suffers from inadequate mechanical isolation of the calorimeter head. The aluminum block and attached cold source are suspended from the center of a thin (approx. 1/16 in.), non-reinforced, stainless-steel deck plate (22.5 × 19.5 in.). This arrangement of a heavy weight mounted in the center of a thin metal plate tends to behave much like a drum head; a loud shout close to the metal deck causes a pen deflection.

In view of the preceding difficulties, certain modifications of the DSC-2 were carried out which allow it to perform rapid, routine measurements on its most sensitive range of 0.1 mcal sec^{-1} at scan rates of 10°C min^{-1} over a −35 to 100°C temperature range with flat, noiseless baselines.

Figure 5 shows the modified portion of the DSC-2. The original aluminum sample holder block was combined with a brass subplate and massive brass cold finger (2 1/2 in. diameter and 5 1/2 in. long) to form a new head assembly. This new head is mounted on the DSC-2 so that it remains continually submerged in a low temperature bath, but at the same time allows immediate access to the sample holders. The original metal deck was replaced with a 1/2 in. thick linen-reinforced laminated phenolic plate* which provides high mechanical strength plus very desirable insulating qualities. An antechamber for the head is provided by a phenolic tube* (5 1/2 in. ht. × 6 in. O.D. × 3/4 in. wall thickness) bolted underneath the deck. The head assembly is mounted into the antechamber by bolting the phenolic tube to the brass subplate of the head. Each interface in the assembly is sealed with low-temperature silicone O-rings**, and each interface in the heat train is coated with Wakefield Thermal Compound No. 128*** to insure efficient heat conduction.

*A.A.A. Plastics, Boston, Mass.
**Irving B. Moore Corp., Cambridge, Mass.
***Wakefield Corp., Wakefield, Mass.

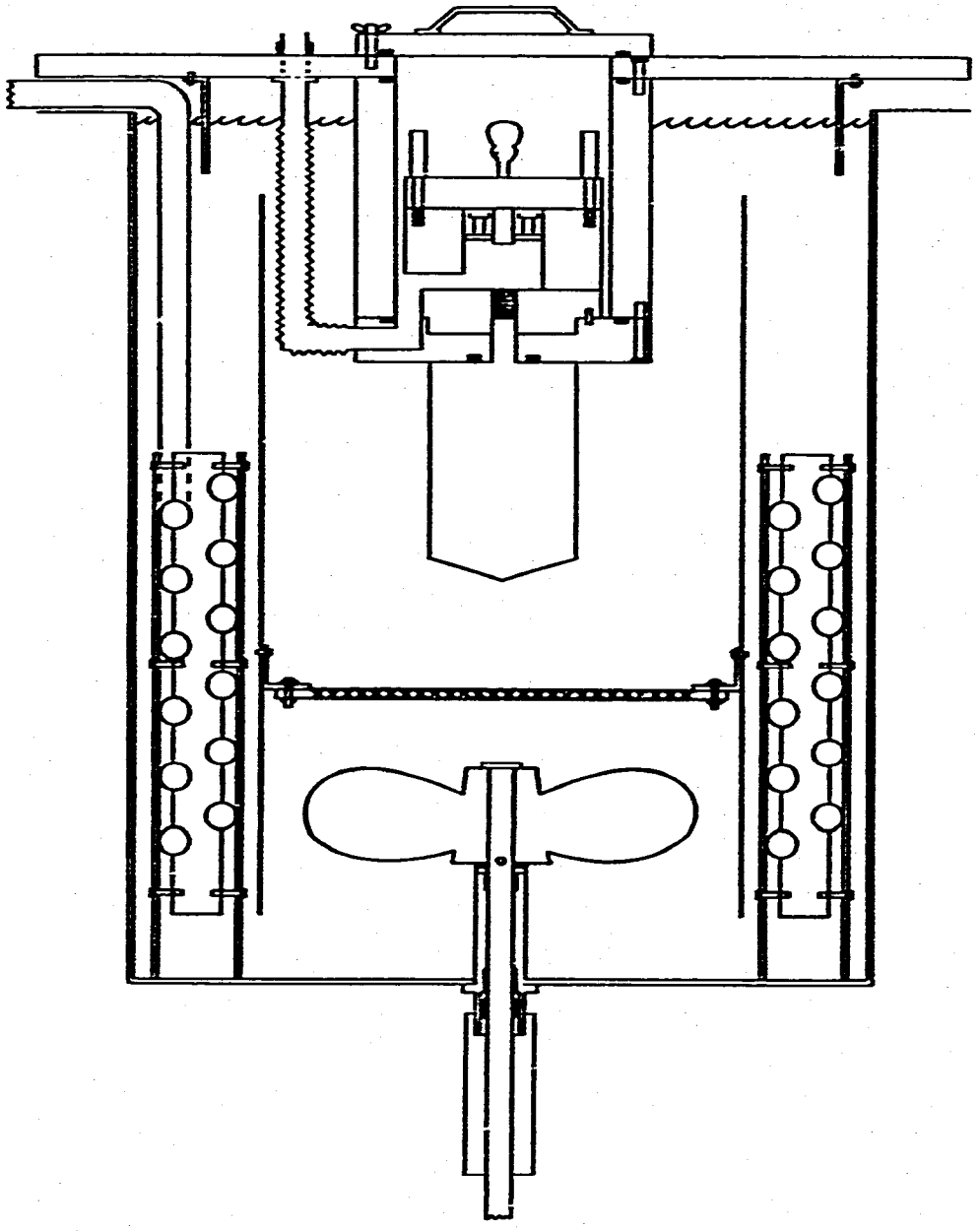

Fig. 5. Schematic diagram of the modified portion of the Perkin-Elmer DSC-2. The original thin metal deck has been replaced by a thick linen-reinforced laminated plate to whose underside a splash ring is mounted. The calorimeter head-cold finger assembly is immersed in the low-temperature bath. A phenolic tube provides an antechamber for the submerged head. The cold temperature bath is shown with its cooling coils, flow-directing internal cylinder, dispersing screen and stirring propeller with sealed low temperature drive train.

The cold finger and block assembly is cooled in a 15 gallon cylindrical stainless steel tank (20 in. ht. by 15 in. diam.) containing 14 gallons of 70% ethylene glycol–water. Another stainless steel cylinder (18 in. ht. by 10 in. diam.) is placed inside the tank (1 1/2 in. clearance from the bottom) to direct the coolant flow upward, bathing the cold finger. A double thickness screen is mounted inside the inner cylinder to disperse uniformly the upward coolant flow and prevent vortex formation. The bottom of the tank is equipped with an 8 in. polycarbonate boat propeller and stainless steel drive shaft and thrust bushings* mounted within a tubular brass housing. A packing cavity with adjustable packing nut provides a low-temperature seal; the packing is teflon-coated asbestos fiber**. The stirring propeller is driven by a 1/8 horsepower gearmotor (10:1 ratio), with speed adjustment (500 rpm maximum) via a variable voltage transformer, mounted underneath the tank and coupled to the drive shaft by a flexible thermally insulating urethane coupling***. This type of coupling minimizes mechanical and thermal coupling between the motor and propeller drive shaft and also allows easy alignment. The tank sits inside a plywood box insulated with poured polyurethane insulation and mounted on a support table which is mechanically independent of the cabinet supporting the DSC-2 instrument.

The bath contains about 40 ft. of 1/2 in. copper evaporating coils. The refrigeration system is driven by a 1 1/2 horsepower Americold compressor§ with water-cooled condensers. The evaporator uses an automatic expansion valve§§ to regulate the flow of refrigerant to the coils and to also allow operator adjustment of the system back pressure. A heat exchanger precools (via the cold backside line) the line refrigerant before it enters the evaporator. The refrigerant used is Freon 502.

The top of the box holding the refrigerated tank and the underside of the phenolic deck are covered with 1/2 in. foam rubber insulation. A splash ring is mounted on the underside of the deck. When the deck is positioned over the tank these two foam rubber surfaces are compressed together to seal the bath from the room environment.

The commercial Plexiglas dry box included with the subambient accessory is mounted on the phenolic deck. Electrical connections, nitrogen purge lines, and the vacuum pickup tool with its on–off switch are within this dry box. Three types of nitrogen purges are employed: a fast purge to the dry box, a slow purge to the antechamber cavity, and a very uniform slow purge to the sample holders (20 ml min^{-1}). Ultradry nitrogen is required for the holder purge and is obtained by passing the gas through a 36-in. column of P_2O_5. The effluent from this dryer column passes via a pressure reducing diffuser plate to the sample holders and exits into the dry box.

---

*Dixon Corp., Bristol, R. I.

**Devcon Form Pack 1, Devcon. Corp., Danvers, Mass.

***Winfred M. Berg Inc., East Parkway, N. Y.

§Rhode Island Refrigeration Supply, Providence, R. I.

§§Singer Model 204C, Control Co. of Am., Milwaukee, Wisc.

An example of results obtained using this modified DSC-2 is shown in Fig. 6. These scans were performed on a wet sample containing 3 mg dry weight of *E. coli*[25,22] whole cells (wild-type W945, grown at 20°C in M3 minimal medium) suspended in 50–50 ethylene glycol–water. The lower peak, centered at about 5°C, characterizes the living cell and occurs in the lipids of the plasma membrane. Provided the calorimeter is not scanned above physiological temperatures, it is seen to be

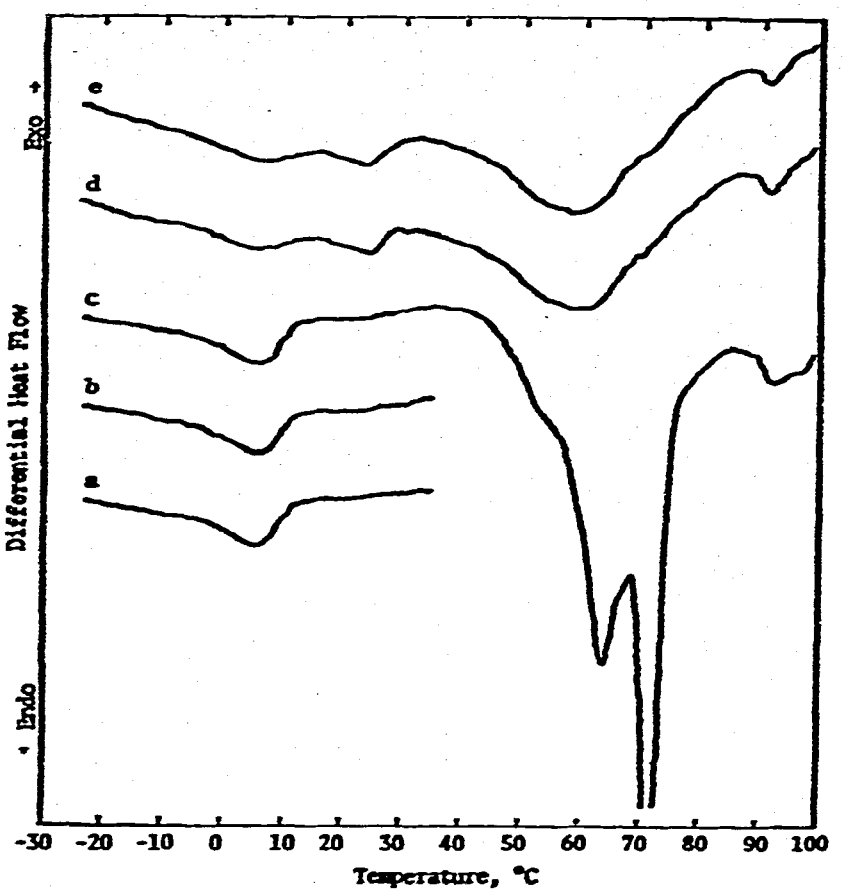

Fig. 6. DSC scans of wild type *E. coli* whole cells obtained with a modified Perkin-Elmer DSC-2. The scans were taken in 50% ethylene glycol (a, b) below protein denaturation temperatures, (c) through protein denaturation, (d, e) and after protein denaturation. In (a–c) the peak centered at 5°C is the cytoplasmic membrane transition. The large peaks in the neighborhood of 60–70°C in (c) are protein denaturation. The peak at 90°C may be DNA. In (d), after heating to high temperature, the cytoplasmic membrane transition remains almost unaltered by tthe outer membrane produces a new peak centered at 25°C. Some protein and possibly DNA peaks remain. Samples were 3 mg dry weight in glycol-buffer. Cells were grown at 20°C in minimal medium.

reversible (Fig. 6a, b). In Fig. 6c the cells are heated to 100°C; in addition to the plasma membrane transition at 10°C, protein denaturation peaks are observed in the neighborhood of 60–70°C. The peak at 90°C may be DNA. A scan taken after heating (Fig. 6d) reveals minor changes in the first transition and shows a new

transition arising from the lipid of *E. coli*'s outer membrane, centered at about 25°C. The peak remaining in the neighborhood of 60°C is reversible protein denaturation, possibly arising from partially re-annealed peptide. Subsequent heatings do not change this pattern (Fig. 6e).

EXAMPLES OF DSC APPLIED TO MODEL SYSTEMS AND BIOMEMBRANES

Model systems

A model system that has been used extensively in biology for permeability studies is produced by the prolonged sonication of phospholipids in water. This process forms small (a few hundred Å diameter), closed vesicles whose walls consist

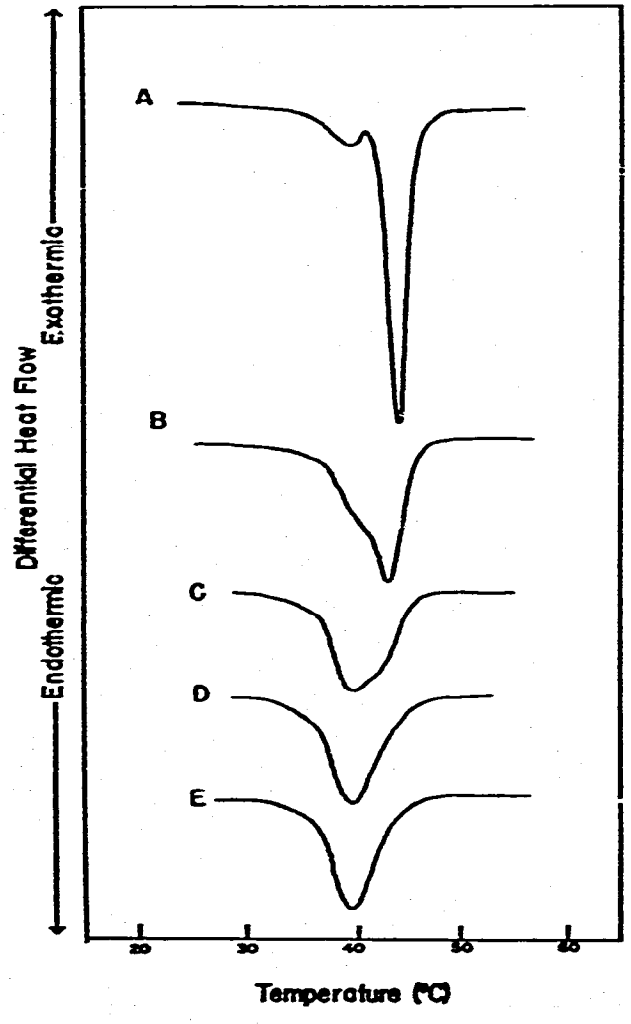

Fig. 7. DSC scans of dipalmitoyl lecithin (A) unsonicated, and (B) sonicated at 50°C for 5 min, (C) 10 min, (D) 21 min, and (E) 38 min. In unsonicated lecithin the characteristic "premelt" appears as a small, lower temperature peak.

of a single bilayer[26]. The use of these vesicles as models for membrane bilayers is questionable since, most likely due to their small radius of curvature[15,27], the molecular packing in these particles is different from the molecular packing in normal lipid bilayers. The similarity of the molecular packing in these particles to the molecular packing in lipid bilayers was debated for about six years with arguments primarily based on Proton Magnetic Resonance[28]. Use of DSC makes the dissimilarity obvious.

Sonication drastically changes the nature of the melt seen in synthetic and naturally occurring lipids alike[15,22,29]. When a dispersion of lecithin or natural lipids is converted to small vesicles, its large endotherm is lowered in temperature, decreased in enthalpy and entropy, and increased in width. This broadening of the transition is also seen by dilatometry[27] and by fluorescent probes[30,29]. The course of sonication can be followed by DSC and reveals the growth of a broad lower temperature endotherm characteristic of the small vesicles at the expense of the higher-temperature endotherm associated with the unsonicated lamellar phase (Fig. 7). Judged calorimetrically, the conversion of the lamellar phase to the vesicular form appears to approximate a two-state process, where, in the intermediate stages of sonication, endotherms characteristic of both states are present. The observed changes necessarily imply a change in the organization of the phospholipid molecules upon sonication. Probably as a consequence of the abnormal packing of lipids in sonicated vesicles if held below their transition temperature, they coalesce with time and their transitions revert to those of unsonicated versicles. The instability of this system below its transition illustrates the importance of being able to scan down in temperature.

Biomembranes

Temperature strongly affects the fatty acid composition of membrane lipids in almost all organisms. The melting points of fatty acids biosynthesized or selected from the growth medium for incorporation into membrane lipids decreases markedly with decreasing growth temperature. This response is required to maintain the membrane bilayer in a liquid state at any temperature[22]. Although formation of membrane lipids is enzymatic, the temperature-responsive control of those fatty acids and hence the position of the membrane transition may not be enzymatic in nature. In studies on *A. laidlawii*, DSC combined with standard biochemical techniques suggests that the temperature sensor and selector of appropriate fatty acids is the lipid bilayer itself.

Aliquots of cells whose membrane transition was characterized by DSC (Fig. 8a) were incubated at various temperatures for a short length of time with a mixture of ^{14}C-labeled palmitic acid ("high-melter") and ^{3}H-labeled oleic acid ("low-melter"), and the amounts of the two fatty acids incorporated into the membrane lipids were measured. A plot (Fig. 8b) shows the results: the palmitate/oleate ratio increasing with temperature. The shape of the curve follows the membrane transition, which is a direct indication of the physical state of the membrane. In studies on protein-free lipid extracts of *A. laidlawii* lipids (Fig. 8c), the ratio of the

physical binding of these fatty acids to the lipid bilayers mimics the selective process in live cells.

This ability to act as a temperature sensor and selector may be a general property of any phospholipid bilayer. Figure 8d is a thermogram of bilayers formed from a mixture of 20% egg lecithin in synthetic dipalmitoyl lecithin, lipids not found in the membrane of *A. laidlawii*. The same transition dependency of the binding of "low-melter" to "high-melter" is seen.

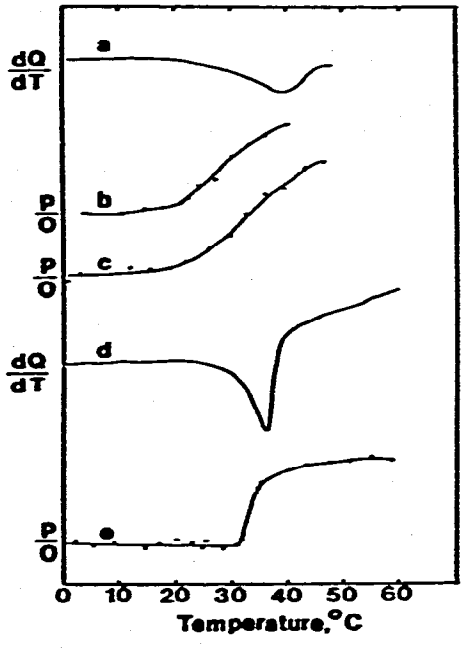

Fig. 8. The bilayer as a temperature-sensing selector of fatty acids. (a) Is a DSC scan of membranes from *A. laidlawii* grown at 37°C in tryptose. The ratio of palmitate to oleate (P/O) taken up from the medium and esterified to the membrane lipids after short-time incubation at various temperatures is shown in (b). Physical binding of palmitate and oleate to protein-free lipids is shown in (c). A mixture of dipalmitoyl lecithin and egg lecithin (20%) produced the DSC scan shown in (d) and fatty acid binding curve in (e).

DIFFERENTIAL SCANNING DILATOMETRY

The success of DSC in the study of biological membranes suggested that the complementary technique of dilatometry might be equally useful. Dilatometry is usually a very tedious procedure which often lacks sensitivity or is restricted in applicability. For this reason a sensitive, automated differential scanning dilatometer (DSD) has been constructed in our laboratory[31]. This device continuously determines the buoyant mass of biological samples as small as a few milligrams, isothermally or as a function of temperature. As in any differential instrument, many errors are implicitly self-corrected and the number of operations is reduced to a minimum. Because this instrument has a resolution of 0.02 μl and is capable of using a large amount of

sample (10 ml maximum volume), it is very suited to measure the broad thermal events seen in biomembranes and other biological materials.

The dilatometer

The dilatometer employs the principle of buoyant density. The sample is contained within a submerged cell and is balanced by an identical reference cell. A Cahn recording electrobalance* provides the sensor for the dilatometer, which appears schematically in Fig. 9. Hanging the sample and reference cells from opposite ends of the beam, each equidistant from the pivot, allows the balance to respond to the

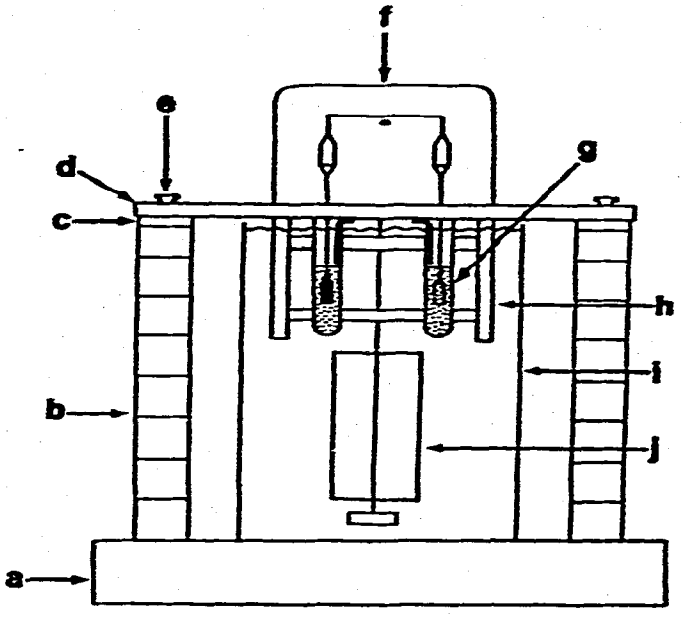

Fig. 9. Schematic diagram of the differential scanning dilatometer: (a) terrazzo base; (b) brick support pillars; (c) aluminum caps; (d) aluminum crossbeam; (e) leveling screws; (f) electrobalance; (g) reference or sample tube; (h) adjustable tube rack; (i) water bath; (j) four-vaned paddle.

difference in mass between sample and reference rather than to the absolute mass of either. If the component parts of the two cells and their suspension systems have identical masses, the electrobalance feeds no signal to its associated recorder. Similarly, if both cells are completely filled with the same liquid of density ρ and are also suspended in the liquid that fills them, the same buoyant force is exerted on each. The recorder then remains at zero, regardless of the temperature or the nature of the suspending medium. On the other hand, if a sample of dry mass m and apparent partial specific volume ϕ is dissolved in the liquid within the sample cell but not within the reference cell, a mass of liquid $m\phi\rho$ is displaced by the sample. The electrobalance continues to ignore the masses of the sample and reference cells and responds

*No. 2000 RG Electrobalance, Cahn Division, Ventron Inst. Corp., Paramount Calif.

only to the buoyant mass of the sample, given by

$$m_b = m(1-\phi\rho) \tag{1}$$

Providing the sample and reference cells are identical and the solvent inside and outside the cells are also identical, the volumes of the cells are unimportant and need not be defined. Since in practice the masses of the materials comprising the two cells are not perfectly matched, a baseline of sample cell run against reference cell is subtracted from actual runs (a very small correction).

In our laboratory the dilatometer is ordinarily operated in the temperature-scanning mode. The differential design adapts it particularly well to scanning, which yields a continuous record of m_b against temperature if the temperature dependence of the solvent density ρ is known. For water, this latter parameter exists in the published literature; for other buffers, it can be obtained from the dilatometer itself. When rearranged, eqn (1) affords the apparent partial specific volume $\phi(T)$ from $m_b(T)$:

$$\phi(T) = \frac{[m-m_b(T)]}{[m\rho(T)]} \tag{2}$$

A computer facilitates calculating both $\phi(T)$ from eqn (2) and the coefficient of expansion $\alpha(T)$ according to eqn (3)

$$\alpha(T) = \frac{1}{\phi}\left(\frac{\partial\phi}{\partial T}\right)_p \tag{3}$$

The detailed construction of this instrument has been discussed elsewhere[31]. Figure 9 illustrates the basic components of the dilatometer, and Fig. 10 provides a detailed view of the sample cell assembly. The design and development of the DSD required that great care be taken to eliminate vibrations and non-uniformity of heat distribution.

The dilatometer temperature and rate of temperature change are regulated by heaters controlled by a proportional temperature controller equipped with a linear programmer. Down-scans are carried out by back-heating the dilatometer bath against a heat sink of cooled water of programmed temperature circulated through copper tubes lining the brass water bath walls. A system of timers and relays permits total automation for repeated up and downscans. Outputs of the electrobalance and sample temperature are monitored by a two-pen chart recorder.

Sample preparation

An extremely important consideration in the dilatometer operation is the removal of dissolved gas. The volume changes investigated generally lead to changes in apparent mass of the order 1–10 mg over a 50°C temperature range. If an air bubble of 1 mm diameter were to form in or on the sample or reference cell in the course of a run, its volume would be about 5.2×10^{-4} ml. Since this volume represents a buoyant force of approximately 0.5 mg, it is important that the system be thoroughly

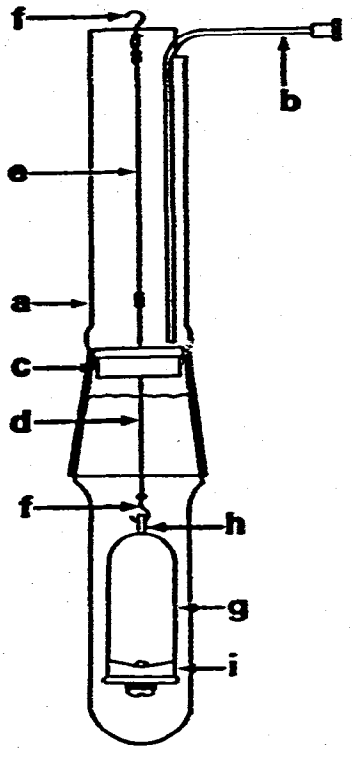

Fig. 10. Complete assembly of sample cell, suspension wire, and glass tube, with purge line in place: (a) Pyrex tube; (b) purge line; (c) plastic insert; (d) tungsten suspending wire; (e) monofilament nylon thread; (f) platinum hooks; (g) reference or sample cell; (h) cellulose nitrate tube; (i) polystyrene cap with neoprene O-ring and nylon sealing screw.

deaerated initially and be prevented from reaerating during the course of a run. Loading the sample and reference cells therefore requires these cells, as well as their suspending liquid, be free of dissolved gas. In loading, the cells are deaerated, loaded with degassed sample suspension or buffer, and sealed under thoroughly degassed water. The cells are then suspended in tubes of degassed solvent (Fig. 10) and the entire tube assembly is placed in a vacuum desiccator for a final deaeration. When the tubes are mounted on the dilatometer rack they are constantly purged with neon to prevent reaeration during a run and to carry away any vapors, thus preventing condensation on the suspension wires.

Dry weight

Using the DSD and above procedures, the largest error in partial specific volume determinations was found to arise from dry weight determinations. The exact meaning of dry weight in materials as complicated as biological membranes is not at all clear. In many biological preparations tightly bound water may not be removed if drying is not sufficiently vigorous, but on the other hand harsh treatment can cause decomposition or loss of other materials in addition to water. In order to

assure accuracy and reproducibility, we have developed an apparatus that allows the sample mass to be monitored continuously under well-defined conditions of temperature and pressure[32]. It is based upon a design described in the literature[33], but is modified to enable determinations to be made faster and more simply than the published design allows.

Briefly, a Cahn electrobalance identical to the one used in the DSD is placed in a vacuum case having a long tube in which the sample pan hangs. A vacuum is maintained while pressure is monitored on a chart recorder using a vacuum thermocouple gauge. Heat from an infrared lamp radiating through the tube wall heats a blackened sample pan in which the sample is contained. This pan is covered with a top having a small hole for the escape of vapor. The arrangement allows heat to be transferred to the sample through conduction rather than radiation so that variations in the color of samples do not affect the "true" temperature at which they are dried. The temperature is controlled by regulating the lamp voltage using a full-wave phase-firing controller whose probe is mounted next to the sample pan. A continuous record of weight is provided by feeding the electrobalance output to a chart recorder. Recordings can easily be made to ± 1 μg in the course of a drying. Temperature is

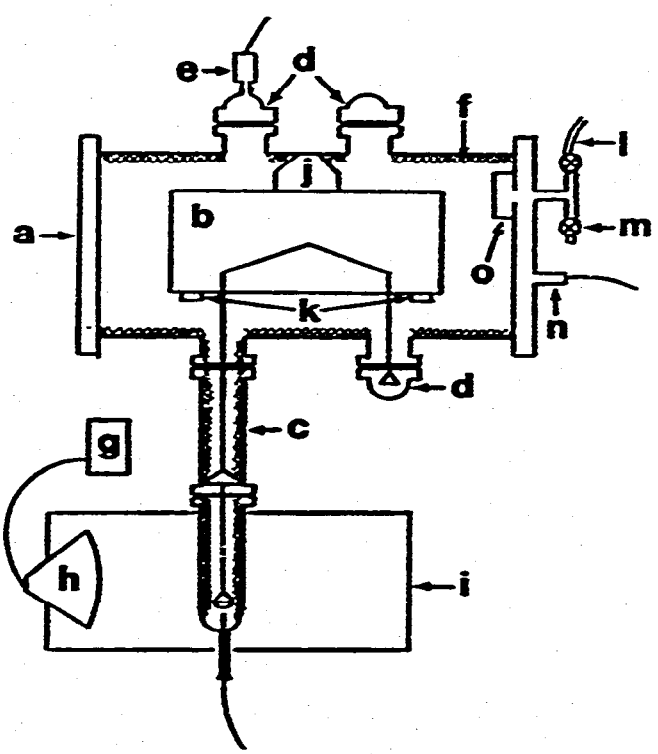

Fig. 11. Schematic diagram of dry weight apparatus: (a) vacuum case; (b) electrobalance; (c) sample tube assembly; (d) domes; (e) vacuum thermocouple gauge; (f) grounded copper screen; (g) temperature controller; (h) infrared heating lamp; (i) oven; (j) metal spring; (k) aluminum support bars; (l) outlet to trap and vacuum pump; (m) bleed; (n) electrical feedthrough; (o) baffle.

monitored by a separate thermister probe mounted immediately under the sample pan and calibrated with respect to the temperature on the inside wall of the sample container.

The basic structure of the dry weight apparatus is shown in Fig. 11. The main vacuum case (a) is an 8 in. diameter Plexiglas cylinder with 1 in. thick walls. The ends are closed by 1 in. thick Plexiglas sheet secured by bolts to a collar of the same plastic fused to the cylinder. Neoprene O-rings in a machined groove provide a tight seal. Openings into the cylinder corresponding to the loop positions on the balance beam are provided by 2 in. diameter acrylic tubes machined to fit snugly into the main cylinder wall into which they are fused. Collars made from Plexiglas sheet are fused to the outer ends of these outlets and grooved to receive an O-ring from a standard 57 mm OD glass flat flange joint. Glass domes (d) fashioned from such joints seal these openings. The bottom dome encloses the stirrup pan from loop C of the electrobalance, while those on top close ports which are not in use. One of the top domes has an inlet for the vacuum thermocouple gauge (e) which monitors pressure within the case.

The vacuum case (a) and sample tube assembly (c) are lined with a grounded copper screen (f) which guards against potentially troublesome static charge. The Cahn balance (b) is held firmly in place in the vacuum case by a metal spring (j) mounted on the top, and aluminum bars (k) screwed to the bottom of its frame. A plastic baffle (o) is mounted over an opening in the end cap to which a glass T joint is fitted. One end of the T joint (l) connects to a needle valve which leads to a liquid nitrogen trap and vacuum pump. The other end of the joint (m) is a bleed, and consists of a needle valve leading to a drying tube. An electrical feed-through (n) carries the wires for the balance, the ground, and the temperature controller probes. The sample tube assembly (c) fits into a hole in an oven (i) constructed of an insulated, tin plated steel can enclosing a 250 W infrared heating lamp (h). The output of the lamp is controlled by a full-wave phase-firing controller (g) whose sensor is within the sample tube assembly (c).

Figure 12 is a detailed illustration of the sample tube assembly. The tube itself (a) is made from two 14 cm lengths of 57 mm O.D. glass flange joints. The grooved flanges of the upper and lower sections are joined at a neoprene O-ring (h) and supported by springs (k) attached to brass rings (j) encircling the glass tubes. These springs can be unhooked to permit easy removal of the bottom tube for access to the sample stirrup (e) which hangs from a long nichrome wire (c) suspended from loop A of the electrobalance. A conical piece of thin aluminum sheet (d) inserted in the upper section of the sample tube assembly acts as a heat deflector and is pierced by a 0.5 cm diameter hole to admit the hanging wire.

The grounded copper screen of the vacuum case is continued down the sample tube assembly (b) with the front section of the screen in the lower tube open at the level of the stirrup (e). The sample pan (f), which sits on the stirrup, is formed from aluminum foil coated on one side with black enamel paint and oven cured at 180°C. These pans are 25 mm in diameter and can hold about 1.5 ml. An aluminum foil lid (g)

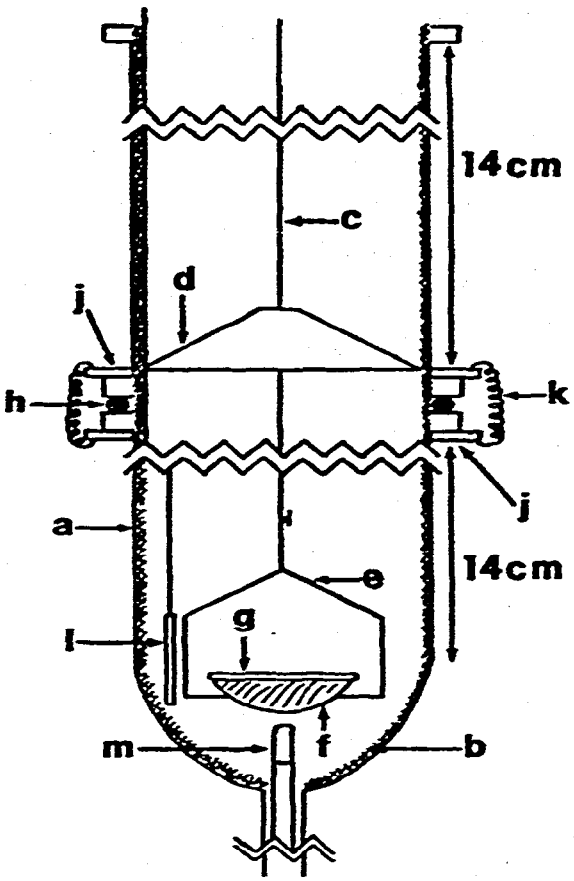

Fig. 12. Sample tube assembly: (a) glass tube; (b) grounded copper screen; (c) nichrome wire; (d) heat deflector; (e) electrobalance stirrup; (f) sample pan; (g) sample pan lid; (h) neoprene O-ring; (j) brass rings; (k) springs; (l) sensor for temperature controller; (m) thermister probe.

with a 1 mm hole in its center is placed over the sample pan during the run to protect the sample from radiant heat and to support the calibrating weight during standardization of the instrument. The temperature controller probe (l) is positioned immediately to the side of the stirrup (g) and the temperature sensor probe (m) is positioned immediately below the stirrup and sample pan. The latter probe was calibrated by means of substances of various melting points to give the actual pan temperature.

In an actual dry weight determination a 1.00 ml sample containing about 5 to 10 mg of material is pipetted into a previously tared sample dish and placed under slight vacuum in a desiccator over silica gel overnight. All samples have been found to dry to a solid during this time without creeping over the edge of the dish. The pan is then transferred to the sample stirrup using grounded metal tweezers and covered with the lid. The sample tube assembly is closed, the vacuum pump, is turned on, and the oven slid into place. The temperature controller is activated while the recorder continuously traces the sample weight while heating in vacuo. A final weight can be

taken without returning the system to atmospheric pressure and temperature. Standard operating conditions are 400 μ pressure and 105°C. When the weight has shown no change over a 20-min period, the sample is considered dry. Most samples reach equilibrium in less than 2 h.

Representative results

Dilatometer performance was tested with two well-defined standards, a 1.00% solution of KCl, and n-eicosane. For KCl, the standard deviation of the experimental points about a sixth-order curve fitted to the same points over the temperature interval of 0–50°C was 0.00007 ml g^{-1} or 0.02%[31]. Accuracy was estimated over the entire temperature range by comparing published values of ϕ with the experimental best-fit curve. The standard deviation for the difference was 0.0008 ml g^{-1} or 0.22% for ϕ at 20°C. Coefficients of expansion, obtained from the best-fit volume curves, are less accurate than the volume measurements themselves; errors of 2–3% could be expected routinely. Similar results were obtained for n-eicosane. At 30°C the experimental ϕ was 1.0756 compared to the literature value[35] of 1.0749. The melting of this hydrocarbon at 35°C appeared experimentally as a 19.0% increase in volume, agreeing well with the literature value 19.3%.

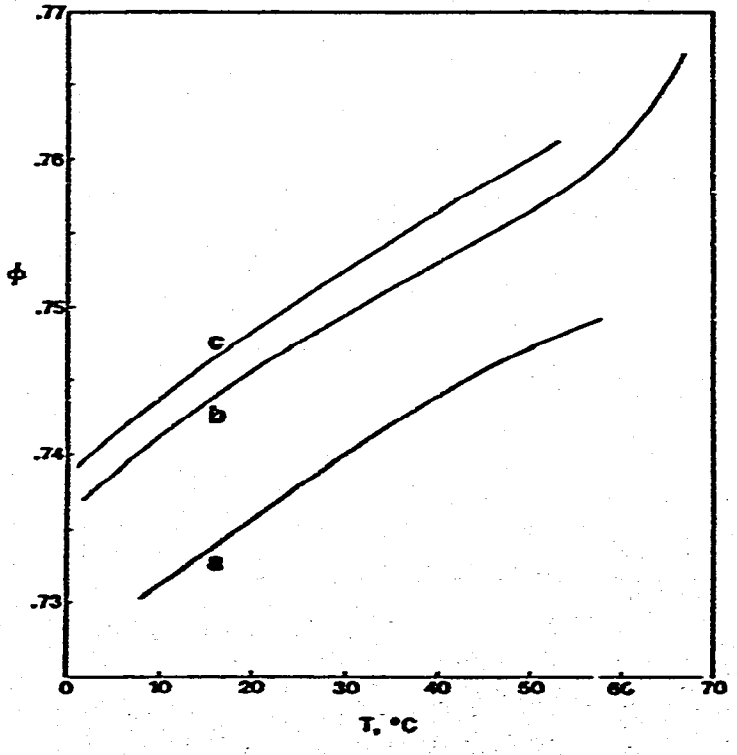

Fig. 13. Apparent partial specific volumes of bovine serum albumin and ovalbumin versus temperature: (a) native bovine serum albumin; (b) native ovalbumin; (c) heat-denatured ovalbumin. Units of ϕ are milliliters per gram.

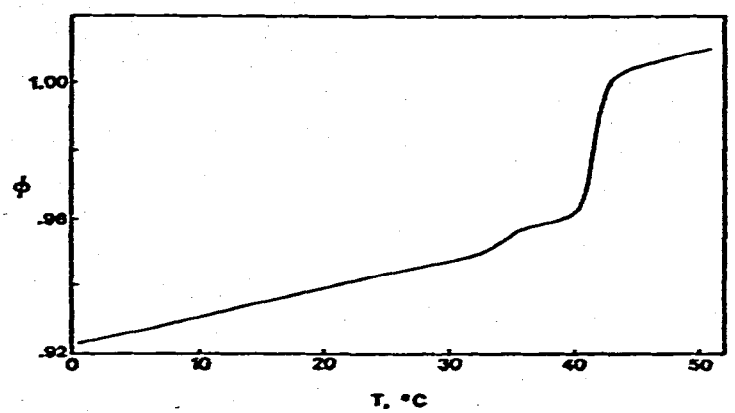

Fig. 14. Dilatometric upscan of dipalmitoyl L-α-lecithin, apparent partial specific volume versus temperature. Units of ϕ are milliliters per gram.

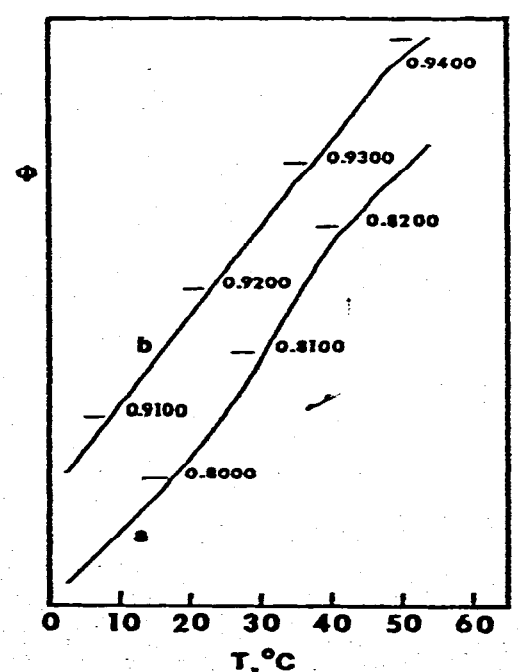

Fig. 15. Apparent partial specific volumes of (a) *A. laidlawii* and (b) calf brain myelin. *A. laidlawii* shows a 2.1% increase in ϕ over its membrane transition.

Dilatometer upscans of two proteins, bovine serum albumin and ovalbumin, are shown in Fig. 13. For these measurements as well as those to be discussed below, about 100 mg dry weight of material was run in deionized water. For bovine serum albumin the ϕ vs. T curve (a) is nearly linear. Native ovalbumin, having a higher ϕ than bovine serum albumin, exhibits a volume increase upon thermal denaturation (b). Both ϕ and α are greater for denaturated ovalbumin (c) than for the native protein.

Figure 14 is an upscan of L-α-dipalmitoyl lecithin (DPL). A thermogram of this lipid is shown in Fig. 2b. Both the chain melt of the lecithin bilayer at 41.5°C and the premelt at 35°C can easily be seen. In downscans the premelt is displaced down in temperature by several degrees, a phenomenon also observed by DSC. The volume change through the transition is 3.5%.

Figure 15 shows upscans of two membranes; (a) *A. laidlawii* and (b) myelin prepared from calf brain. In *A. laidlawii* the membrane transition is seen as a 2.1% increase in volume. The small concavity seen in the curve from 40–50°C is most likely protein denaturation. Since the membrane of *A. laidlawii* is about 50% lipid and 50% protein, its partial specific volume is intermediate in value between that of lipid and protein. The higher ϕ of myelin reflects its high (ca. 80%) lipid content.

No transition is seen in myelin due to its high content of cholesterol, which allows bilayers to exist over a wide temperature range in a semi-fluid state without undergoing a transition[22]. The concavity observed from 35 to 47°C is well above noise level and is reproducible.

An additional example of the application of DSD to biology will be given in the last portion of this paper. It should be noted now, however, that the dilatometer frequently reveals details in thermal profiles which cannot be detected in the DSC (and vice versa), so that the two methods complement each other nicely. And unlike DSC, the dilatometer gives a unique and characteristic curve for every substance.

THERMAL STUDIES OF SERUM LIPOPROTEINS

An ongoing study of the human serum lipoproteins illustrates the advantages of approaches which integrate several different but complementary thermoanalytical methods. The serum lipoproteins, which constitute a major component of blood plasma, are particles consisting of lipids solubilized by association with proteins[36]. Neither the state of the lipids within the particles nor the mode of association of the lipids with the proteins is well understood. Their primary function seems to be the transport and exchange of lipids, and from time to time they have been suggested to play a role in arteriosclerosis. They are usually divided into four major classes defined by density ranges (chylomicrons, very low density, low density, and high density) which are usually isolated by ultracentrifugal flotation in buffers whose densities are adjusted by adding salt. With the exception of some overlap between chylomicrons and the very low density lipoproteins, classes have characteristic flotational coefficients and are distinct from one another. The exact lipid composition of each class varies from sample to sample but for each, it falls within a specific range

characteristic of the class. Similarly, although the protein composition of each class is heterogeneous and some proteins are shared in common, each class seems to be characterized by a unique and constant spectrum of proteins.

Of the four classes of serum lipoproteins, we are concerned with only two, the low density lipoproteins (LDL) and the high density lipoproteins (HDL). Both of these classes are structurally more interesting and present a more challenging problem than the chylomicrons or the very low density lipoproteins, which appear to be essentially fat droplets. The LDL contain about 25% protein, and 75% lipid consisting of phosphatides, cholesteryl esters, cholesterol, and triglycerides. The HDL consist of approximately equal amounts of protein and lipid. The lipid of HDL has a higher proportion of phosphatides and a lower cholesteryl ester component than the lipid of LDL. Except for fatty streaks in arterial walls, the high cholesteryl ester content characteristic of the LDL and HDL is not found elsewhere in biology.

An extensive arsenal of biochemical and biophysical techniques have been applied to the lipoprotein problem, but a satisfactory structural model remains elusive. The apolipoproteins, especially those of the HDL, have been reasonably well characterized biochemically, and the amino acid sequences of some are known. NMR studies indicate that the bulk of the lipids are not tightly bound to the apoprotein, but appear to be highly mobile[37]. The helical content of both the HDL and the LDL is appreciable, and the secondary conformation of their proteins appears to be more temperature labile than that of most other proteins[38–40]. Both spectroscopic

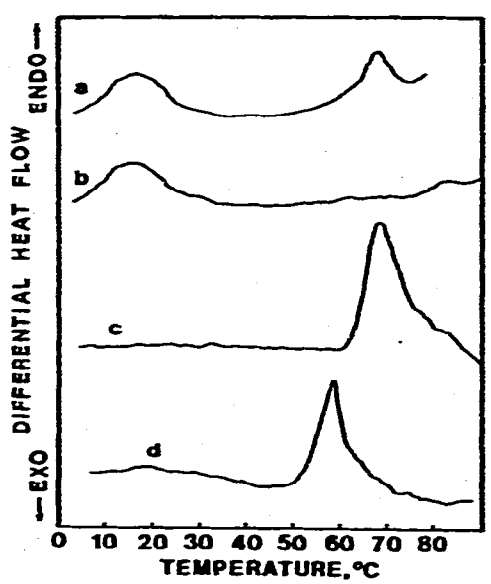

Fig. 16. DSC scans of human low-density serum lipoproteins (a) in their native state before thermal protein denaturation and (b) after protein denaturation, and of human high-density serum lipoproteins (c) before and (d) after protein denaturation. The scans differ considerably, the LDL showing a low-temperature peak arising from a lipid transition and irreversible protein denaturation, but the HDL showing no lipid peak and reversible protein denaturation. All samples were dissolved in phosphate-buffered saline at pH 7.4 and scanned at 10°C per minute.

and chemical evidence suggest that much of the protein and the polar ends of the phosphatide molecules are accessible to solvent, a conclusion consistent with thermodynamic arguments. Much of the physical and chemical evidence is, in general, consistent with a lipid core rich in cholesteryl esters, bounded by phospholipid molecules and peripheral protein, although recent X-ray diffraction studies have been interpreted to suggest the presence of a lipid bilayer and a central core of protein[41].

The thermal profiles of the LDL and the HDL, shown in Fig. 16, differ considerably from each other. Both reveal some unexpected features. A reversible transition occurs in the LDL, centered at about 15°C, which is unaffected by thermal protein denaturation. The protein peak, at about 70°C, is irreversible. Superficially, the behavior of the LDL in the DSC resembles that of biomembranes (compare Figs. 3 and 4). However, in spite of the considerable phospholipid content of the LDL, the lower temperature peak appears to correlate with the transition temperature of extracted cholesteryl esters (probably the nematic/isotropic transition) rather than with the temperature expected for phospholipid bilayers[42]. No separate lipid bilayer transition can be detected. If the observed reversible transition can in fact be assigned to cholesteryl esters, the structural implications are obvious: within the lipoprotein particle is a pool of cholesteryl ester large enough to behave thermally like bulk esters. The most likely location is in the core of the particle.

No reversible lipid transition, from either cholesteryl esters or phospholipid bilayers, can be detected in the HDL by DSC. Apparently, in spite of the fact that the cholesteryl ester content is still appreciable (about 50% of the lipids in the LDL and 30% in the HDL), a pool large enough to melt is not present. Careful determinations of the heat of the lipid transition seen in the LDL should enable us to determine the percentage of the cholesteryl esters in the LDL which contribute to the peak. If all contribute, the LDL and HDL may represent quite different structures, but if only half contribute, the thermally inactive half may exist in the same state in both lipoproteins. The proteins in the LDL and HDL also appear to behave quite differently. As pointed out, protein denaturation in the LDL is irreversible, as it is in many other proteins, and the protein peak disappears after the sample is heated to high temperatures. In the HDL, on the other hand, a large reversible protein peak remains after heating but occurs at a lower temperature than in the native material. The major proteins in the HDL and LDL differ chemically, and DSC studies of the lipid-free apolipoproteins from both classes should clarify whether the peculiar denaturation profile in the HDL is characteristic of the proteins themselves or a result of lipid–protein interaction.

The results of the combined techniques of DSC, dilatometry, and circular dichroism are shown in Fig. 17 for the LDL. The DSC of the lipoprotein is essentially the same as in Fig. 16, although the lipid peak occurs at a slightly higher temperature. The protein peak is unchanged. Different donors gave the two samples, and the discrepancy is a result of different fatty acid compositions. The general temperature course of the apparent partial specific volume is as expected: there is a nearly linear increase with temperature, similar to that observed in other proteins (see Fig. 13).

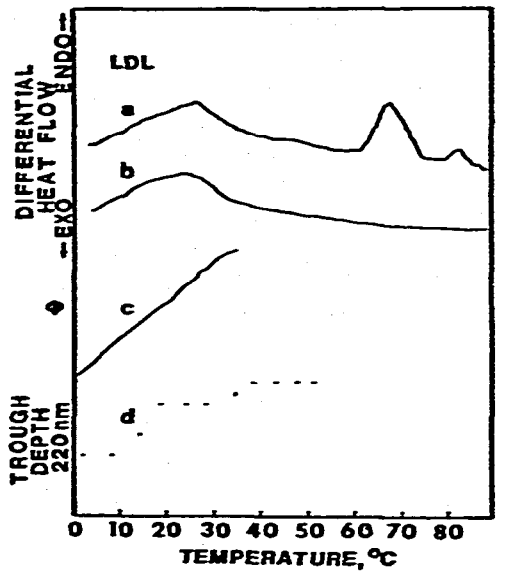

Fig. 17. Calorimetry, dilatometry, and circular dichroism of human low-density serum lipoproteins. The DSC scans of (a) native and (b) heat-denatured materials are essentially the same as shown in Fig. 16. The sample is from a different donor, and the slightly elevated lipid transition temperature reflects a change in fatty acid composition. Fine structure in the curve of apparent partial specific volume (c) may arise from protein conformation changes not detected by the DSC. CD does in fact indicate (d) such changes do occur. The small wiggles in DSC scans (a) and (b) are instrumental noise. The wiggles in DSD scan (c) are well above background noise and are reproducible.

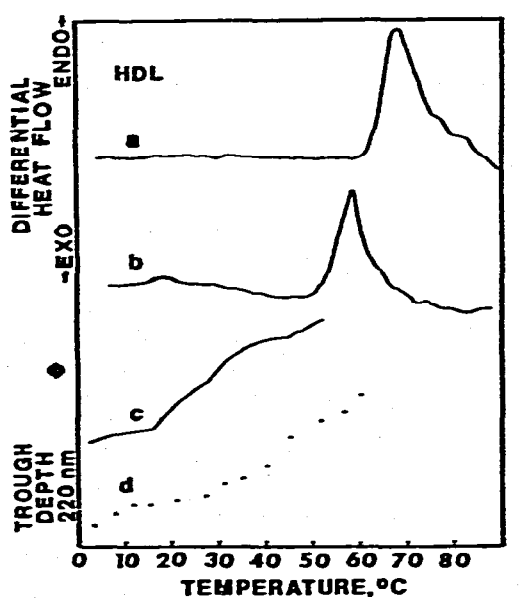

Fig. 18. Calorimetry, dilatometry, and circular dichroism of human high-density serum lipoproteins. The DSC scans, shown earlier in Fig. 15 are of (a) native and (b) heat-denatured materials. The thermal behaviour of the apparent partial specific volume (c) differs considerably from that of the LDL, and suggests a glass transition. CD again indicates (d) that minor protein conformational changes occur, but are not detected by DSC, below the temperature of major protein denaturation.

The decrease in slope at the upper end of the curve may indicate the completion of the lipid melt, as it does in *A. laidlawii* shown in Fig. 15a. If this is true, much of the volume change up to 35°C may arise from the cholesteryl ester transition; additional dilatometer scans to higher temperatures are necessary. Superimposed upon the curve are several small inflections which could reflect minor lipid transitions but more likely arise from protein transitions. The CD curve verifies that such transitions in secondary protein conformation do indeed occur at temperatures below those ordinarily associated with protein denaturation. CD studies of LDL of varying fatty acid composition, and hence varying cholesteryl ester transitions, will determine whether the protein conformation changes are independent of the lipid transition.

Like the DSC scans, the dilatometer scan of the HDL (Fig. 18) is far different from that of the LDL. The behavior seen in Fig. 18b is quite unexpected, and cannot arise from a first-order lipid transition since none is seen in the DSC. Such behavior, a sharp discontinuity in the coefficient of expansion, has not been seen in other systems and is strongly reminiscent of a glass transition. The presence of a glass transition might be verified by other methods such as NMR or DSC. It is not surprising that no accompanying discontinuity in the heat capacity is seen in Fig. 18a. Both the dilatometry and the CD were carried out under near-equilibrium conditions, with very slow heating and cooling, while thermal cycling was rapid in the DSC (10°C per minute). Since glass transition temperatures are very dependent upon thermal histories, DSC must be operated in the appropriate mode to give genuine C_p measurements. The secondary protein conformation of the HDL, like that of the LDL, is revealed by CD to be thermally labile at temperatures below massive denaturation, although the changes are not as pronounced as they are in the LDL.

Although the results described here are preliminary and are included largely to illustrate the value of a thermoanalytical approach to biological problems, a consistent interpretation seems to be emerging. In contrast to previous results obtained by isothermal measurements, thermoanalytical methods strongly suggest that the LDL and HDL are fundamentally quite different particles. If these first impressions are sustained by subsequent work, the different physical properties could imply different biological roles.

ACKNOWLEDGEMENTS

We gratefully acknowledge support for portions of this work from the Leukemia Foundation, Inc., NIH Postdoctoral Fellowship No. 5 FO2 GM55229 and U S P H S GM20545. The authors thank Mr. G. Carnegis, Mr. H. A. Klos, Mr. J. Hall, Mr. R. Brandon, and Mr. R. Holburn for their valuable assistance.

REFERENCES

1 E. Overton, *Vierteljahrsschr. der Naturforsch. Ges.* (Zurich), 44 (1899) 88.
2 E. Gorter and F. Grendel, *J. Exp. Med.*, 41 (1925) 439.
3 J. F. Danielli and E. N. Harvey, *J. Cell Comp. Physiol.*, 5 (1935) 483.

4 F. O. Schmidt, R. S. Bear and K. J. Palmer, *J. Cell Comp. Physiol.*, 18 (1941) 31.
5 J. D. Robertson, in M. Lacke (Ed.), *Cellular Membranes in Development*, Academic Press, New York, 1964, p. 1.
6 E. D. Korn, *Science*, 153 (1966) 1491.
7 D. E. Green and J. F. Perdue, *Proc. Nat. Acad. Sci. USA*, 55 (1966) 1295.
8 A. A. Benson, in L. Boil and B. A. Pethica (Eds.), *Membrane Models and the Formation of Biological Membranes*, North Holland, Amsterdam, 1968, p. 190.
9 J. Lenard and S. J. Singer, *Proc. Nat. Acad. Sci. USA*, 56 (1966) 1828.
10 V. Luzzati in D. Chapman (Ed.), *Biological Membranes*, Academic Press, London and New York, 1968, p. 71.
11 D. G. Dervichian, *Prog. Biophys. Mol. Biol.*, 14 (1964) 263.
12 Y. K. Levine, *Prog. Biophys. Mol. Biol.*, 24 (1972) p. 1.
13 M. C. Phillips, R. M. Williams and D. Chapman, *Chem. Phys. Lipids*, 3 (1969) 234.
14 E. J. Shimshick and H. H. McConnell, *Biochemistry*, 12 (1973) 2351.
15 J. M. Steim, in R. F. Gould (Ed.), *Molecular Association in Biological and Related Systems*, American Chemical Society, Washington, D.C., 1968, p. 259.
16 J. M. Steim, M. E. Tourtellote, J. C. Reinert, R. N. McElhaney and F. L. Rader, *Proc. Nat, Acad. Sci. USA*, 63 (1969) 104.
17 J. C. Reinert and J. M. Steim, *Science*, 168 (1970) 1580.
18 D. L. Melchior, H. J. Morowitz, J. M. Sturtevant and T. Y. Tsong, *Biochim. Biophys. Acta*, 210. (1970) 114.
19 D. M. Engelman, *J. Mol. Biol.*, 58 (1971) 153.
20 J. C. Metcalfe, N. J. M. Birdsall and A. G. Lee, *FEBS Lett.*, 21 (1972) 335.
21 J. M. Steim, in S. A. Van den Berg, P. Borst, L. L. M. Van Deenen, J. C. Riemersma, E. C. Slater and J. M. Tager (Eds.), *Mitochondria/Biomembranes*, North Holland, Amsterdam, London, 1972, p. 185.
22 D. L. Melchior and J. M. Steim, *Ann. Rev. Biophys. Bioeng.*, 5 (1976) 205.
23 J. M. Steim, *Methods Enzymol.*, 22 (1974) 262.
24 P. J. Scheidler and J. M. Steim, *Methods Membrane Biol.*, 4 (1975) 77.
25 G. B. Ashe, Thesis, 1976, Brown University, Providence, Rhode Island.
26 C. Huang, *Biochemistry*, 8 (1969) 344.
27 M. P. Sheetz and S. I. Chan, *Biochemistry*, 11 (1972) 4558.
28 D. Lichtenberg, N. O. Petersen, J. L. Giradet, M. Kainosho, P. A. Kroon, C. H. A. Seiter, G. W. Feigenson and S. I. Chan, *Biochim. Biophys. Acta*, 382 (1975) 10.
29 J. Suurkuusk, B. R. Lentz, Y. Barenholz, R. Biltonen and T. E. Thompson, *Biochemistry*, 15 (1976) 1393.
30 J. F. Faução and C. Lusson, *Biochim. Biophys. Acta*, 307 (1973) 459.
31 J. F. Blazyk, D. L. Melchior and J. M. Steim, *Anal. Biochem.*, 68 (1975) 586.
32 To be published.
33 R. Goodrich and F. J. Reithel, *Anal. Biochem.*, 34 (1970) 583.
34 *International Critical Tables*, Vol. III, McGraw-Hill, New York, p. 87.
35 P. R. Templin, *Ind. Eng. Chem.*, 48 (1956) 154.
36 J. D. Morrisett, R. L. Jackson and A. M. Gotto, *Ann. Rev. Biochem.*, 44 (1975) 183.
37 J. M. Steim, O. J. Edner and F. G. Bargoot, *Science*, 162 (1968) 909.
38 D. G. Dearborn and D. B. Wetlaufer, *Proc. Nat. Acad. Sci.*, 62 (1969) 179.
39 A. Scanu, H. Pollard, H. Hirz and K. Kothary, *Proc. Nat. Acad. Sci.*, 62 (1969) 171.
40 A. Scanu, *Biochim. Biophys. Acta*, 181 (1969) 268.
41 L. Mateu, A. Tardieu, V. Luzzati, L. Aggerbeck and A. M. Scanu, *J. Mol. Biol.*, 70 (1972) 105.
42 R. J. Deckelbaum, G. G. Shipley, D. M. Small, R. S. Lees and P. K. George, *Science*, 190 (1975) 392.